

Real-time Phase Detection for EEG-based tACS Closed-loop System

G. Zarubin^{1,2}, C. Gundlach^{2,3}, V. Nikulin² and M. Bogdan¹

¹Technical Informatics Department, Leipzig University, Leipzig, Germany

²Max Planck Institute for Human Cognitive and Brain Sciences, Leipzig, Germany

³Institute of Psychology, Leipzig University, Leipzig, Germany

Keywords: Closed-Loop Stimulation, EEG-tACS, Phase Detection, Oscillations.

Abstract: In this paper, we present a robust and fast implementation of a closed loop EEG-transcranial-alternating-current-stimulation (tACS) paradigm focusing on phase coupling between the tACS signal and alpha-oscillations of the ongoing EEG signal. We provide an evaluation of three phase-prediction methods for alpha oscillations of offline EEG data and for artificially generated oscillations with different noise levels in terms of optimization time as well as accuracy of prediction. Successful functioning of the whole system with delays compensation and data corrections is demonstrated in real-time pilot measurements with humans.

1 INTRODUCTION

Transcranial alternating current stimulation (tACS) is a technique adapted to investigate relationships between oscillatory neuronal activity and behavior. This method allows to non-invasively apply oscillatory currents to the human brain thereby modulating ongoing neuronal oscillatory activity in a frequency-dependent way (Herrmann et al., 2013; Reato et al., 2013). tACS has been successfully used to modulate neuronal oscillatory activity and human brain function in different modalities such as vision (Vossen et al., 2015), motor function (Feurra et al., 2011) or audition (Riecke et al., 2015). There is preliminary evidence that tACS might be effective to support recovery of motor functioning in patients with stroke (Fedorov et al., 2010) or optic neuropathy (Sabel et al., 2011).

Conventional non-adaptive stimulation does not take into account states of neuronal oscillation and their response to stimulation, thereby limiting investigation of mechanisms and efficiency of possible applications. The increasingly prominent field of research using closed-loop EEG-tACS or EEG-TMS models (Thut et al., 2017; Bergmann et al., 2016) aims for a better understanding of the mechanisms of tACS and an enhancement of tACS effects. However, there are several common challenges and limitations, which slow down the development of closed-loop models. One of the main challenges is the difficulty to analyze online effects

due to induction of oscillatory stimulation artifacts in EEG/MEG, that are several magnitudes larger than the measured signals in the EEG. Although, there are some attempts (Witkowski et al., 2015), which may allow elimination of artifacts, such approaches require sophisticated experimental design or heavy computational procedures. Another issue for a closed-loop system is the demand for maximum proximity to real-time functioning to allow for following rapid (millisecond range) dynamics of brain oscillations, which imposes additional restrictions on both technical equipment and data processing methods. Moreover, the whole set up of such system requires a broad technical knowledge and is, therefore, not easily adaptable for clinical applications.

In this paper, we present a robust and fast implementation of a closed loop EEG-tACS paradigm focusing on phase coupling between the tACS signal and alpha-oscillations. The alpha rhythm is prominent brain rhythm linked to many brain functions such as perception, attention and working memory (Jensen et al., 2010; Foxe et al., 2011) and which was previously successfully modulated by tACS (Helfrich et al., 2014; Vossen et al., 2015). Our closed loop EEG-tACS model incorporates different methods and concepts to overcome above-mentioned challenges. In the methods section, we describe our general model scheme and methodological framework. Further, in the results section, firstly, we provide an evaluation of three phase prediction methods based on offline alpha oscillations and

artificially generated waves with different noise levels in terms of optimization time as well as four metrics for accuracy of prediction. Secondly, we demonstrate successful functioning of our system with delays compensation and data corrections based on pilot measurements from first real-time experiments. Finally, in the discussion section, we consider the properties of our model, future directions for development and further extended experimental investigation implementing our closed-loop system to answer questions about tACS mechanisms and parameters to yield optimal stimulation effects.

2 METHODS

To perform real-time experiments with phase prediction and adaptive stimulation our system should be capable of precise, reliable and fast data processing. Besides, an essential part of the implementation of closed-loop systems is the minimization and compensation of computational (time for extraction and prediction of signals according to predetermined relation to brain state) and technical (signal transmission between devices and interfaces) delays. We used an intermittent protocol with separated sliding windows for EEG acquisition and stimulation that had two modes of phase relation between alpha band and tACS-signal implemented – in-phase and anti-phase. In order to satisfy the condition of real-time functioning and minimize computational delays - we implemented our model with all data processing procedures in C++ language and performed compensation of phase shift based on required optimization time.

2.1 General Model Scheme and Definition of Elements

The proposed model consists and works in terms of following parts (Figure 1):

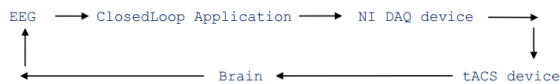


Figure 1: General model scheme.

where EEG represented by brain activity recorded with BrainProducts amplifier, ClosedLoop Application – by program in C++ with BCI2000 (Schalk, 2004) module for data acquisition, NI DAQ device – by National Instrument USB 6343 for transmitting stimulation signal on tACS stimulator input, tACS – by neuroConn DC-Stimulator Plus.

The model is implemented with 3 different modes of functioning – “Online”, “Offline”, “Record-only” / “Stimulation-only”. In “Online” mode (Figure 2) the system functions in a state required for adaptive stimulation - in short interval cycles (e.g. 1 sec) and incorporates: import of EEG signals (imaging or pre-stimulation interval), estimation of optimal parameters (e.g. phase shift) and stimulation signal, computation of required optimization time, actual compensation of optimization and transduction delays and transmission of stimulation-signal (stimulation interval) through NI DAQ card to stimulator device input (BNC port). A setting for a typical experiment also includes post stim interval for analysis of effects and inter trial interval.

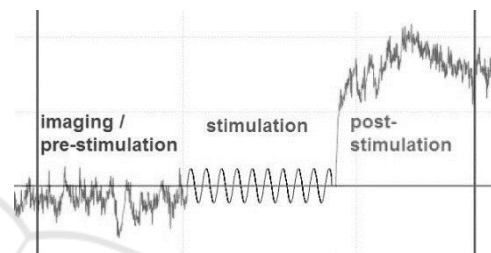


Figure 2: “Online” mode, data from pilot measurement, sampling rate 500 Hz, 1 trial, EEG data from Oz channel, length of all intervals – 1 sec, vertical lines here and later represent borders of trials.

“Offline” mode is used for testing optimization methods and procedure on predefined datasets of real and artificial EEG, therefore, it has only imaging and stimulation intervals. In “Record-only” mode EEG signal is recorded and saved for further analysis. In “Stimulation-only” mode particular number of stimulation signals with predefined fixed parameters are transferred to stimulator. This mode – non-adaptive stimulation – that can be used for comparisons with adaptive stimulation mode.

Our application allows choosing between 2 modes of phase relations with respect to the neuronal control signal: “in-phase” (minimal phase lag), “anti-phase” (phase lag close as possible to π) and 3 methods for phase prediction: 1) Phase prediction (Hilbert based) (PP), 2) Phase prediction using Autoregression model (PP on AR), 3) Zero Crossing (based on Butterworth zero-phase filtering) (ZC). The evaluation of methods with offline data is based on 4 measures: 1) Relative accuracy (based on relation to optimally possible stimulation), 2) Degree Deviation (from optimal phase), 3) Phase Locking Value (PLV), 4) Phase Synchrony (based on entropy).

2.2 Phase Prediction Methods

2.2.1 Phase Prediction (Hilbert based)

In general, measurements of neural oscillations demonstrates variable phase dynamic, because of complex source signals and volume conduction effects (Nolte et al., 2004; Nikulin et al., 2011). However, if we analyze short time intervals we can consider phase dynamics to be quasi stationary. This assumption allows us to perform phase prediction by extraction of phase from a current (imaging or pre-stimulation) interval in order to forecast phase dependent stimulation for the following interval. Importantly, we include only a predefined part of the imaging interval for phase extraction (extraction interval), which is controlled by a parameter and is usually represented by the second half or last quarter of the whole interval. For the extraction interval, phase values should be optimal to achieve better prediction. We used Hilbert transformation (with FIR filtering) and iterative search across sinusoidal waves with different phases for this optimization. Euclidean difference (L^2 norm) for vectors of instantaneous phase between extraction interval and various generated sine-waves were criteria for minimization – in case of “in-phase” relation, maximization – in case of “anti-phase” relation.

2.2.2 Phase Prediction using Autoregression Model

Autoregressive (AR) models are a class of linear predictive techniques. They attempt to predict the signal sample based on previous signal samples by using the AR parameters as coefficients and additional noise component. The number of samples used for prediction determines the order of the model. The AR parameters can be estimated by different techniques such as Kalman filter, Yule-Walker, Expectation-Maximization, Least-square. We implemented AR model based on a modified Burg Maximum Entropy method (Bourke et al., 1998), the order of AR model was chosen as half of the length of imaging interval. AR model was applied for prediction of data of the stimulation interval. Precisely, we perform prediction only for the first part of stimulation interval (AR interval), where the exact proportion is controlled by a parameter. Similarly to the previous method, the AR interval is used for determining phase by an iterative optimization of generated sine waves and with Hilbert-transformed data of the interval. Afterwards, optimal phase is assigned to the whole stimulation interval.

2.2.3 Zero Crossing (Based on Butterworth Zero-phase Filtering)

Another possible approach for phase prediction is related to the analysis of the last zero crossing point of the filtered signal (Wilde et. al, 2015). Most of conventional filters produce phase shift into the filtered data. One of the ways to eliminate this issue is processing the input data in both forward and reverse directions. We implemented an algorithm similar to the Matlab `filtfilt()` function, which, after filtering the data in the forward direction, reverses the filtered sequence and runs it back through the filter; the result has zero phase distortion and doubled order of the filter. There are two possible scenarios with analysis of the last zero crossing point – transitions from negative to positive and the opposite (“- +”, “+ -”). In both cases we calculate the distance from zero crossing to the end of interval (“- +”: “a”, “+ -”: “b”), for “in-phase” relation: in “- +” scenario phase shift can be approximated by the value of “a”, in “+ -” by “ $\pi + b$ ”; for “anti-phase” relation: in “- +” by “ $\pi + a$ ”, in “+ -” by “b”.

2.3 Evaluation Metrics

2.3.1 Relative Accuracy

The phase of neural oscillations is always not clearly expressed due to noise in measured signals and rapid fluctuations of brain activity and states (Freyer et. al, 2009), therefore, the evaluation of the prediction methods requires some relative measure. In case of short quasi stationary intervals, we can estimate accuracy by comparison the predicted forecasted phase and the actual “optimal” phase of the stimulation interval. “Relative accuracy” (RA) is determined as a relation of differences (Euclidean distances) of instantaneous phase vectors. For “in-phase” relation (1):

$$RA(\text{in}) = \frac{\Delta_{\text{optimal}}}{\Delta_{\text{predicted}}} * 100, \quad (1)$$

for “anti-phase” (2):

$$RA(\text{anti}) = \frac{\Delta_{\text{predicted}}}{\Delta_{\text{optimal}}} * 100, \quad (2)$$

where $\Delta_{\text{predicted}}$ is the difference of instantaneous phase values for predicted wave and data from stimulation interval, Δ_{optimal} – difference of instantaneous phase values for optimal wave (for stimulation interval) and data from that interval. For “in-phase” relation, the optimal wave is defined as sinusoidal wave with minimum difference of

instantaneous phases between this wave and EEG data, for “anti-phase” as a sinusoidal wave with maximum difference. Figure 3 illustrates the “Relative accuracy” measure and provides a comparison of results for the three phase prediction methods on the one interval.

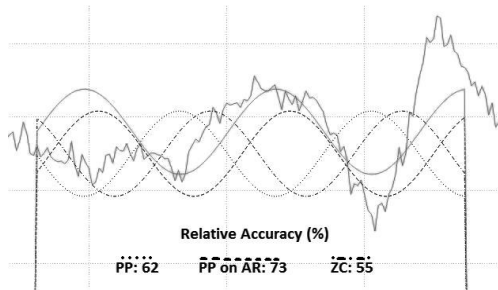


Figure 3: Relative Accuracy metric values, “in-phase” relation, ¼ sec interval, EEG data, dot line: “Phase Prediction (Hilbert based)” / PP , dash line : “Phase prediction using Autoregression model” / PP on AR, dot dash line: “Zero Crossing” / ZC, solid line: “optimal” phase.

2.3.2 Degree Deviation

After we determined the optimal phase shift for stimulation interval and phase shifts predicted by different methods, we can calculate the “Degree Deviation” (DD) for predictions (3):

$$DD = |\delta_{\text{pred}} - \delta_{\text{opt}}| * 360^\circ / \frac{Sr}{Afr}, \quad (3)$$

where δ_{pred} , δ_{opt} are predicted and optimal phase shifts, Sr the sampling rate frequency and Afr the alpha frequency. For our purposes, phase coupling has only two important modes: “in-” and “anti-” phase, therefore, we can consider the “Degree Deviation” $DD > 180^\circ$ as $DD = 360^\circ - DD$. In case many trials are available for the calculation of “Degree Deviation”, the statistical deviation is determined to estimate stability of prediction method as well as dynamics of phase changes for oscillations.

2.3.3 Phase Locking Value

The Phase Locking Value (introduced for neural signals by Lachaux et al., 1999) - defined at time t as the average value (4):

$$PLV_t = \frac{1}{N} \left| \sum_{n=1}^N e^{j\theta(t,n)} \right|, \quad (4)$$

where $\theta(t, n)$ - the instantaneous phase difference: $\varphi_1(t, n) - \varphi_2(t, n)$, n - trials. PLV measures the intertrial variability of this phase difference at t : if the

phase difference varies little across the trials, PLV is close to 1; otherwise it is close to 0.

2.3.4 Phase Synchrony

Another measure to investigate the relation between oscillations is phase synchrony, based on entropy and was proposed by (Tass et al., 1998). We can consider series of instantaneous phase differences, obtained from the Hilbert transform of two intervals, and build a histogram of their distribution on a number of phase bins for $[-\pi, \pi]$. For two sinusoidal waves, the histogram should be centered around one bin, for two random signals, the histogram should span across all bins. Using the concept of Shannon’s entropy we can calculate the entropy for the histogram (5):

$$H = - \sum_{k=1}^N P_k \ln(P_k), \quad (5)$$

where P_k can be approximated as relative frequency of phase difference for k -th bin (value of k -th bin divided by number of all points in histogram). Then, the Phase synchrony index can be estimated as (6):

$$\gamma = \frac{H_{\text{max}} - H}{H_{\text{max}}}, \quad (6)$$

where $H_{\text{max}} = \ln N$, and N is the total number of phase bins. The phase synchrony γ is normalized in interval $[0..1]$, where γ closer to 1 reflects the signals with high synchrony, and γ close to 0, reflects low synchrony.

2.4 Compensation of Optimization and Transduction Delays

Optimization delays are estimated by C++ object *QElapsedTimer* as a difference between time points before start and after finishing the optimization. The transduction delay is estimated by averaging the time differences across all trials between the last signal before the actual start of stimulation in raw EEG data (from BrainProduct Recorder) and the last signal in the imaging interval from the ClosedLoop Application minus optimization delay. For compensation, the total delay divided by *factor* (where *factor* = 1000 / sampling rate) is added to the phase value. To dismiss artifacts caused by transduction delay in post-stim interval, after the stimulation function was executed, we skip a number of points equal to the transduction delay divided by *factor*. For a further analysis of possible effects, we need to consider all data before the exact start of stimulation. Therefore, after the optimal phase was determined, we shifted data in the imaging interval to the left (on number of points equal to the total delay

divided by *factor*) and added new signals, received during optimization and transduction delays.

3 RESULTS

3.1 Evaluation of Phase Prediction with Artificially Generated Data

An analysis of performance was conducted on artificially generated signals with different levels of noise. Every level is represented by different signal-to-noise (SNR) ratios, which were measured as the ratio of the signal power to the noise power. A sequence of 10 stimuli (1 sec duration for imaging and stimulation intervals, ¼ sec for extraction and AR intervals, AR data filtered by 12 Hz low pass FIR filter with length 24 samples, FIR filter with length 40 samples for Hilbert transform in “PP” and “PP on AR”) was created based on a composition of 4 sin waves and random Gaussian noise (7):

$$A * \sin(4.3) + A * 1.5 * \sin(9.0) + \\ + A/2 * \sin(20.0) + A/2 * \sin(32.2) + T * Gn \quad (7)$$

where A, T – amplitude coefficients, G_n – Gaussian noise with $\mu = 0.0$, $\sigma = 0.5$). Results are presented in Table 1. The “Relative Accuracy” metric was excluded, because when increasing noise level, the difference between instantaneous phase values of generated data and slightly different sinusoidal waves will wane, producing even higher “Relative Accuracy” results for more noisy data. Optimal phase shift for “Average Degree Deviation” was determined on data without noise and used for further comparison with noisy signals. Results show that even in the case of high noise level for two methods (“PP”, “PP from AR”) “Average Degree Deviation” does not significantly differ from optimum of a noise-free signal. Moreover, prediction from autoregression

data have slightly less deviation, whereas prediction based on zero crossing gives considerably worse results. “PLV” and “Synchrony Index” show similar linearly decreasing dynamics for all three methods. Importantly, here, one point or minimal step (8) for phase shift is 6.48° ($Sr = 500$ Hz, $Afr = 9$ Hz) :

$$step = 360^\circ / \frac{Sr}{Afr}, \quad (8)$$

“Synchrony Index” even for signals without noise gives significantly lower values, because of high entropy level for histogram of phase differences between data represented by composition of several sin waves and data represented by single sin wave.

3.2 Evaluation of Phase Prediction with Offline EEG Data

An analysis of phase prediction methods with offline EEG data was performed on the LEMON dataset (Babayan et. al, 2018) (resting state eyes closed / eyes opened, 64 channels, 2500 Hz, resampled to 500 Hz). Individual alpha frequency (IAF) was determined for each subject before analysis as a contrast of FFT amplitude spectra of eyes-open and eyes-closed data. The IAF value was used as stimulation frequency. Performance of methods for forecasting the exact alpha phase was evaluated on data from channel Oz with different pre-stimulation time lengths from 100 ms to 500 ms; prediction for longer intervals is not reliable due to unstable dynamics of alpha phase even in closed eyes state. In all cases imaging and stimulation intervals were equal to the time window, whereas extraction and AR interval were set to ¼ part of the time window. Length of the FIR filter for “PP” and “PP on AR” was 1/12 of the time window. For “ZC” a Butterworth 2nd order 8-13 Hz band pass filter was used. Table 2 and Table 3 present the average results for 8 subjects, “in-phase” and “anti-phase” relations, eyes closed state, sequence of 20 stimuli.

Table 1: Results of phase predictions for simulated EEG data: 1 sec, 10 stimuli, “in-phase” relation.

SNR (dB)	Average Degree Deviation (°)			PLV			Synchrony Index		
	PP	PP fr. AR	ZC	PP	PP fr. AR	ZC	PP	PP fr. AR	ZC
no noise	19 ± 7	17 ± 6	38 ± 4	0.931	0.931	0.931	0.527	0.517	0.528
5.8	22 ± 9	14 ± 6	37 ± 5	0.907	0.907	0.906	0.471	0.469	0.476
2.8	23 ± 9	12 ± 6	38 ± 7	0.841	0.841	0.840	0.390	0.387	0.403
1.03	18 ± 11	11 ± 6	39 ± 5	0.759	0.760	0.759	0.326	0.320	0.337
-1.18	18 ± 13	9 ± 6	45 ± 4	0.603	0.604	0.601	0.250	0.244	0.258
-2.64	25 ± 18	11 ± 9	49 ± 5	0.479	0.481	0.478	0.214	0.206	0.219
-3.73	26 ± 18	14 ± 1	52 ± 8	0.390	0.392	0.389	0.193	0.193	0.200
-5.33	33 ± 18	21 ± 17	56 ± 9	0.280	0.282	0.280	0.187	0.175	0.187

Table 2: Results of phase predictions for eyes closed, Oz channel, “in-phase” relation, 8 subjects, 20 stimuli.

time window (ms)	Average Relative Accuracy (%)			Average Degree Deviation (°)			PLV			Synchrony Index		
	PP	PP from AR	ZC	PP	PP from AR	ZC	PP	PP from AR	ZC	PP	PP from AR	ZC
100	67	68	72	67	85	83	0.652	0.645	0.643	0.393	0.415	0.397
200	77	84	77	62	70	91	0.627	0.626	0.622	0.318	0.333	0.321
300	79	86	78	58	68	94	0.623	0.623	0.621	0.304	0.313	0.308
400	81	88	83	66	70	85	0.575	0.575	0.574	0.294	0.296	0.284
500	80	88	81	69	66	88	0.583	0.582	0.583	0.302	0.294	0.292

Table 3: Results of phase predictions for eyes closed, Oz channel, “anti-phase” relation, 8 subjects, 20 stimuli.

time window (ms)	Average Relative Accuracy (%)			Average Degree Deviation (°)			PLV			Synchrony Index		
	PP	PP from AR	ZC	PP	PP from AR	ZC	PP	PP from AR	ZC	PP	PP from AR	ZC
100	83	73	77	118	109	82	0.633	0.647	0.639	0.371	0.393	0.385
200	87	80	78	96	77	94	0.622	0.623	0.622	0.345	0.344	0.339
300	90	83	78	74	63	90	0.621	0.623	0.621	0.344	0.342	0.340
400	92	82	80	79	75	85	0.575	0.575	0.574	0.316	0.309	0.304
500	92	85	81	71	72	89	0.582	0.582	0.583	0.331	0.333	0.326

The results prove the feasibility to predict the stimulation signal in determined relation based on an intermittent procedure. Actual phase prediction accuracy is difficult to evaluate, because phase of neural oscillations is not always clearly expressed and changes rapidly.

Similarly to artificial EEG data with increasing noise level, “PLV” and “Synchrony index” linearly decrease when the length of the time window increases. In contrast, “Average Relative Accuracy” values increase with the length of the window, which can be explained by the fact, that for longer intervals the alpha oscillations show more fluctuations. Therefore, optimal phase for the whole interval will be less predictable and may vary across parts of the interval, which means that the difference between optimal and predicted waves will be less. For this metric, in case of “anti-phase” “PP” has higher values, because it is based on the maximization of phase values differences and this maximization is in general more typical for unstable alpha behaviour than concurrence of phases for minimization in case of “In Phase” relation. “Average Degree Deviation” mostly shows higher values for “ZC”. In general, “ZC” produces less accuracy, because it is based on representing the data in only one point, where particular configuration of sign and distance from that point to the end of interval strongly depends on filter parameters. Moreover, if phase shifts happen in the

interval after the last zero crossing, the prediction by this method is likely not to forecast the new phase properly. The evaluation of the methods based on this data did not identify a single best method for the stimulation, both “PP” and “PP on AR” may thus be used for experiments. Additional broader studies with different data sets and more subjects are required for better investigation of presented methods.

3.3 Optimization Time

Average optimization time for different methods and windows are presented in Table 4. A sequence of 50 stimuli was used for evaluation, extraction and AR interval in all cases was set to ¼ part of time window. All calculations were performed on Lenovo P70, Intel i7 OctaCore 2.6GHz, 16Gb RAM.

Table 4: Results in terms of required optimization time (ms), average values across 50 stimuli.

time window (ms)	PP	PP from AR	ZC
100	8.95	9.17	0.18
200	9.18	9.23	0.2
300	9.27	9.31	0.22
400	9.45	9.55	0.24
500	9.8	9.87	0.25
1000	10.6	12	0.34

The time for “PP” and “PP on AR” are almost equal, because both methods are based on iterative optimization with Hilbert transform; autoregression prediction requires very short time, less 1 ms, and does not change a lot by increasing the interval. The order of AR was always set to the half of the imaging interval. ZC works significantly faster, since it only uses filtering and performs prediction based on analysis of sign and distance from one single point. The values allow to use all methods for real-time processing and compensate optimization delays without losing alpha phase dynamics.

3.4 Pilot Measurements and Delay Compensations

In pilot measurements with 3 participants, we performed 8 blocks of 50 stimulation periods – 4 blocks with open eyes and 4 with eyes closed. In every block there were equal numbers of “in-phase” and “anti-phase” relations in random order. The imaging, stimulation and post-stim interval were 1 sec, extraction and the AR interval were set to ¼ sec, the inter-trial interval was random [range: 333 to 666 ms] with mean value of 500 ms. “PP” was chosen as a method for phase prediction, 1 mA value for stimulation was used in all cases. Data from the first pilot measurement allowed us to estimate the transduction delay, which was on average 72 ms, and was used for compensation of phase prediction and for correction of data in imaging and post-stim intervals.

4 DISCUSSION

In this paper we presented a framework for a closed-loop EEG-tACS system, which is ready for the application in experimental investigations of tACS mechanisms and effects. We implemented an intermittent approach for in-phase and anti-phase stimulation in alpha band, evaluating three phase prediction methods in terms of four metrics and required computational time. Using stimulation-free intervals for extraction and prediction of phase values allowed us to avoid stimulation artifacts. Results of the phase prediction for short intervals with offline EEG data demonstrated the feasibility of such an approach, allowing to reliably keep the predetermined phase relation even with rapid alpha phase dynamics. Analysis of performance for simulated EEG data testified robustness of the used methods even with high noise levels. Short optimization times for all methods allows the model to be used for stimulation

in real-time adapted to ongoing alpha oscillations. Successful delay compensation, data corrections and functioning of the whole system was proven by pilot measurements.

There are several crucial points in our model, which determine the direction of further development. Firstly, with the current hardware configuration in total we still have a relatively long delay between end of imaging and the start of the stimulation interval: around 73-85 ms, which may, in the case of alpha oscillations, represent a whole cycle. One possible solution which we are currently developing depends on using another amplifier with shorter delay in signal acquisition, such as NeurOne from Bittium, which, by transmitting data through Ethernet protocol with small delays, is more suited for real-time applications. Another solution is to perform analysis of phase stability for every participant and to develop modification of prediction based on it. Secondly, precise coupling in real-time with neural oscillations parameters (such as instantaneous phase or frequency) requires fast reliable decomposition methods or spatial filters to attenuate volume conduction effects (and thus signal mixing) and to obtain more stable source signals. Therefore, the extraction of phase values from one electrode and using it for stimulation is a slightly restricted strategy. We consider decomposition techniques such as Spatio-Spectral Decomposition (SSD) (Nikulin et al., 2011) as an alternative and promising solution. SSD allows to extract oscillations in particular frequency band even with low signal-to-noise ratio and has few milliseconds running time.

In the last years, the direction of closed-loop brain stimulation has been expanding significantly, especially, for considering exact phase dynamics of ongoing oscillations. In particular, (Mansouri et al., 2017) proposed a short window-forecasting algorithm for phased-locked stimulation using Fast Fourier and Hilbert transformations. They use a similar intermittent protocol with separate windows for the extraction of phase and the prediction of stimulation. However, they consider only two methods for phase prediction, use only one metric for estimation of performance, and have not presented the whole closed-loop system and its functioning. Other examples include attempts to establish closed-loop tACS models based on data prediction from zero crossing of slow oscillations (Wilde et al., 2015), with the help of autoregressive spectral estimation and time-series prediction (Chen et al., 2013), by detecting sleep spindles (Lustenberger et al., 2016) and based on alpha power analysis (Boyle et al., 2013). Certainly, directly comparing methods

presented in this paper and related other methods will be beneficial for the development of closed-loop models and will allow to determine better strategies. However, comprehensive studies on different methods require their implementation in a uniform environment (Matlab or C++) with a similar as possible parameters, performance metrics, data sets and computational power, which was not in the scope of this paper, but is of high interest for our future work.

Investigation of possible effects and mechanisms of adaptive tACS demands broad and deep analysis of data from many participants, different brain states and parameters. The presented model is currently adapted for experiments focusing on potential alpha-phase-dependent effects of closed-loop tACS. According to (Strüber et al., 2015), conventional tACS does not lead to any significant after effects within short intermittent procedure. By using closed loop tACS with an extended number of subjects we want to examine whether phase-locked tACS can produce substantial effects. This work represents an important step towards adaptive tACS and provides a feasible framework for the development of such systems.

REFERENCES

- Babayan A, Erbey M, et al. A Mind-Brain-Body dataset of MRI, EEG, cognition, emotion, and peripheral physiology in young and old adults. Scientific Data (under review), 2018
- Bergmann TO, Karabanov A, et al. Combining non-invasive transcranial brain stimulation with neuroimaging and electrophysiology: current approaches and future perspectives. *NeuroImage*, 2016
- Bourke P, Sergejew A, et al. Auto-regression Analysis, <http://paulbourke.net/miscellaneous/ar/>, 1998
- Boyle MR, Frohlich F. EEG feedback-controlled transcranial alternating current stimulation, 2013 6th International IEEE/EMBS Conference.
- Chen LL, Madhavan R, et al. Real-Time Brain Oscillation Detection and Phase-Locked Stimulation Using Autoregressive Spectral Estimation and Time-Series Forward Prediction. *IEEE Trans Biomed Eng.* 2013
- Fedorov A, Chibisova Y, et al. Noninvasive alternating current stimulation induces recovery from stroke. *Restor Neurol Neurosci* 2010
- Feurra M, Bianco G, et al. Frequency-dependent tuning of the human motor system induced by transcranial oscillatory potentials. *J Neurosci* 2011
- Foxe JJ, Snyder AC. The Role of alpha-band brain oscillations as a sensory suppression mechanism during selective attention. *Frontiers in Psychol*, 2011
- Freyer, F., Aquino, K., et al. Bistability and non-Gaussian fluctuations in spontaneous cortical activity. *The Journal of Neuroscience*, 2009
- Herrmann CS, Rach S, et al. Transcranial alternating current stimulation: a review of the underlying mechanisms and modulation of cognitive processes. *Front Hum Neurosci* 2013
- Helffrich RF, Schneider TR, et al. Entrainment of brain oscillations by transcranial alternating current stimulation. *Current Biology*, 2014
- Jensen O, Mazaheri A. Shaping functional architecture by oscillatory alpha activity: gating by inhibition. *Frontiers in Human Neuroscience*, 2010
- Lachaux JP, Rodriguez E, et al. Measuring phase synchrony in brain signals. *Hum Brain Mapp.* 1999
- Lustenberger C, Boyle MR, et al. Feedback-Controlled Transcranial Alternating Current Stimulation Reveals a Functional Role of Sleep Spindles in Motor Memory Consolidation. *Curr Biology*, 2016
- Mansouri F, Dunlop K, et al. A Fast EEG Forecasting Algorithm for Phase-Locked Transcranial Electrical Stimulation of the Human Brain. *Front Neurosci.* 2017
- Nolte G, Bai O, et al. Identifying true brain interaction from EEG data using the imaginary part of coherency. *Clin Neurophysiol* 2014
- Nikulin VV, Nolte G, Curio G. A novel method for reliable and fast extraction of neuronal EEG/MEG oscillations on the basis of spatio-spectral decomposition. *NeuroImage*, 2011
- Reato D, Rahman A, et al. Effects of weak transcranial Alternating Current Stimulation on brain activity – a review of known mechanisms from animal studies. *Front Hum Neurosci* 2013
- Riecke L, Formisano E, et al. 4-Hz Transcranial Alternating Current Stimulation Phase Modulates Hearing. *Brain Stimulat* 2015;8
- Sabel BA, Fedorov AB, et al. Non-invasive alternating current stimulation improves vision in optic neuropathy. *Restor Neurol Neurosci* 2011;29
- Schalk G, McFarland DJ, et al. BCI2000: a general-purpose brain-computer interface (BCI) system., *IEEE Trans Biomed Eng.* 2004
- Strüber D, Rach S, et al. On the possible role of stimulation duration for after-effects of transcranial alternating current stimulation. *Front Cell Neuro* 2015
- Tass P, Rosenblum MG, et al. Detection of n:m Phase Locking from Noisy Data: Application to Magnetoencephalography. *Phys Rev Lett*, 1998
- Thut G, Bergmann TO, et al. Guiding transcranial brain stimulation by EEG/MEG to interact with ongoing brain activity and associated functions: A position paper. *Clinical Neurophysiology*, 2017
- Vossen A, Gross J, Thut G. Alpha Power Increase After Transcranial Alternating Current Stimulation at Alpha Frequency (α -tACS) Reflects Plastic Changes Rather Than Entrainment. *Brain Stimulat* 2015;8
- Wilde C, Bruder R, Binder S, et al. Closed-loop transcranial alternating current stimulation of slow oscillations. *Curr Directions in Biomed Eng.* 2015
- Witkowski M, Garcia-Cossio E, et al. Mapping entrained brain oscillations during transcranial alternating current stimulation (tACS). *NeuroImage* 2015